EM navigation of a Raman spectroscopy needle for prostate cancer confirmation: Preliminary ex-vivo study in 3D Slicer*

Roozbeh Shams[1,2], Fabien Picot[1,2], Guillaume Sheehy[1], Cynthia Menard[2,3], Jean-Francois Carrier[2,3], Frederic Leblond[1,2], and Samuel Kadoury[1,2]

[1] Polytechnique Montreal, Montreal, QC, Canada
[2] CHUM Research Center, Montreal, QC, Canada
[3] Radio-oncology Dept., University Montreal Hospital Center, Montreal, QC, Canada

1 Purpose

The standard of care for prostate cancer (PCa) biopsies and therapies is based on intra-operative TRUS-guided procedures, but this leads to false-negative rates which can go up to 35% [2]. In the particular case of radical prostatectomies, the more exhaustive analysis concludes to 28% of biopsies being actually positive [5]. A promising approach to reduce negative biopsy rates is to take advantage of the highly sensitive and specific optical properties of prostate tissue. Its purpose would be then to provide the urologist or surgeon with molecular information in situ prior to sample collection. Provided in real-time during the biopsy needle insertion, this new data collection may result in more accurate tumor targeting and therefore, decreasing the false-negative rate. Raman spectroscopy (RS) is an optical technology which demonstrated its ability to discriminate malignant from normal tissue and was successfully performed in vivo during brain tumor resections [7]. More specifically to the biopsy guidance issue, a RS probe was developed to enhance lymph-node biopsy guidance [6], while another one was used in vivo in a swines brain during brain biopsy procedure [4]. For prostate cancer, cell lines [9] and snap-frozen [3] tissue were used for Raman studies. More recently, a mesoscopic characterization was made to test if RS was an appropriate tool to diagnose and to grade prostate cancer [1]. In this work, we present a navigation system for RS that can be used in situ prior to tissue extraction to confirm the presence of PCa.

2 Methods

The proposed system includes four main components. 1) Raman spectroscopy system; 2) Electromagnetic tracking system; 3) Transrectal ultrasound imaging (TRUS); 4) Deformable MRI-TRUS registration method. These components were linked together through the 3D Slicer software, as shown in Fig. 1. The goal is to navigate the optical probe to a target identified on the pre-operative MRI, acquire and analyze spectrums to discriminate tissues.

* Supported by Canada Institutes of Health Research (CIHR) funding.

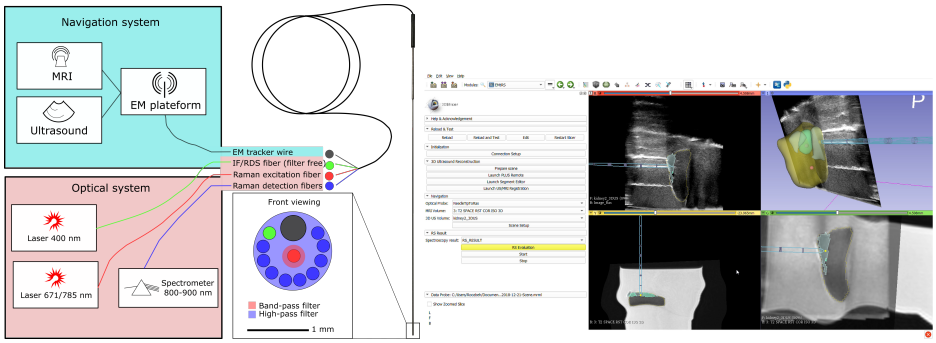

Fig. 1. Left: Components of the system. Right: Screenshot of the navigation environment and visualization of results. Top left: Live 2D ultrasound with the location of the optical probe. Top right: Segmented targets (calyx, medulla and cortex), results of RS, location of the optical probe and ultrasound. Bottom left: Deformed MRI. Bottom right: Deformed MRI in sagittal view.

In order to adhere to the clinical requirements, the diameter of the Raman spectroscopy probe was kept below 1.3mm and its length over 17cm. It is integrated with the EM tracking device which location is 1.75 mm away from the probe's tip. As for the 11 optical fibers shown in Fig. 1, one is used for Raman excitation while 9 of the others are for Raman signal collection. Finally the tip of the probe is covered with two different optical filters, for both excitation and collection purposes. The fibers and tracker wires are gathered in a bundle which is connected to the navigation system and to the optical sources (MCWHL5, Thorlabs) and spectrometer (QE65pro, Ocean Optics) which compose the optical system. The acquisition of the optical data is controlled by a customized Matlab software developed in house. The integration time, laser power and the number of spectra are the parameters to control the synchronization of the laser source and the camera. Once the raw data is collected from a given target, the spectra is processed to extract the Raman signal from the sample. This data processing includes the following steps: background and artifact removal, x-axis calibration, National Institute of Standard and Technology (NIST) correction, fluorescence signal removal and finally normalization by the power source and integration time.

A 5-DOF 0.8mm EM sensor was integrated at the tip to track the location of the optical probe. The transrectal ultrasound probe used in the proposed system is also tracked with a 6-DOF sensor. A 3D ultrasound volume is reconstructed by collecting EM tracked US frames. This tracked volume is used to find the transform between the EM coordinate system and MRI referential. In order to navigate to targets identified on the MRI, the position of the sensors must be in the same coordinate system. For this purpose, we register the MRI volume (T2 sequence) to the acquired 3D US volume with the method mentioned in [8]. This work uses the segmentation of the prostate in both modalities to perform the registration. The processed Raman spectra is then used to build a classification

model based on a Support Vector Machine (SVM) classifier. The purpose of this SVM classifier is to discriminate between normal and cancer tissues, such as between the calyx and the medulla/cortex in the case of the second experiment with slight optical differences.

3 Results

The system was evaluated in both synthetic and ex-vivo models. The first included small cubes of dyed Polydimethylsiloxane (PDMS) with 5mm, 2mm and 1mm in length. The other was a piece of swine kidney. MRI scans of both models were acquired and segmented. For the PDMS-gelatin phantom, the PDMS parts were segmented and identified as targets. For the kidney-gelatin phantom, the calyx, medulla and cortex were segmented. The targets were arbitrary points within all three sub-regions in the kidney. We note that for experiment 1 (using PDMS-gelatin), landmarks were used to register MRI to 3D US since the inclusions were too small to be used for segment registration.

In the first experiment, the probe was navigated to the target area, where RS was performed to discriminate between PDMS and gelatin, while for the second experiment, our goal was to distinguish calyx from cortex and medulla. Due to the pronounced peaks in the Raman spectrum of PDMS and calyx, we were able to detect the target tissue with RS by using the variance of the normalized spectrum. Then, we visualized the result of the RS by color coded spheres on the MRI and 3D space. In these experiments, gelatin and calyx were determined by yellow spheres. PDMS, cortex and medulla were denoted by red spheres. We targeted the three PDMS pieces in Experiment 1 and nine points in Experiment 2. We were able to navigate to and discriminate the 5mm and 2mm PDMS piece but not the 1mm piece. For the second experiment, we successfully navigated to the chosen points and were able to distinguish between calyx and medulla/cortex as shown in Fig. 2. To evaluate the navigation error, the tip location was recorded on the tracked ultrasound. We acquired six positions based on the location of the tracked ultrasound. We also recorded the tip according to the sensor in the needle. The target registration error (TRE) using these six points was 3.7 ± 1.3 mm, but which also included the calibration error from TRUS imaging using a water bath phantom.

4 Conclusion

One of the challenges during prostate biopsy procedures is to confirm the location of cancerous target tumors. We provide a solution by utilizing RS to detect and confirm the location of cancerous tissue. We proposed a framework which includes an EM tracked optical needle, tracked TRUS, MRI/US fusion and RS output visualization in the 3D Slicer environment. We were able to navigate and detect inclusions as low as 2mm in diameter. We also demonstrated the workflow by using a gelatin phantom that included a piece of swine kidney, being able to successfully distinguish calyx from cortex and medulla in the swine kidney. In

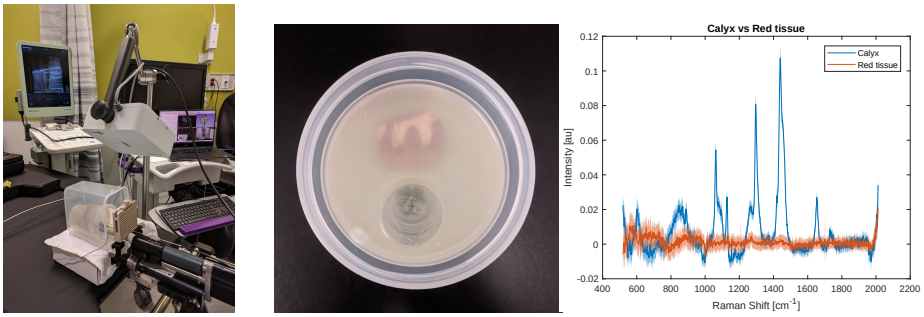

(a) (b) (c)

Fig. 2. (a) Experimental setup. The optical probe, US system, stepper and template along with EM field generator and the phantom can be seen. (b) PDMS-gelatin and kidney-gelatin phantom are shown on the left. On the right, the Raman spectra for PDMS and gelatin is shown on the top. (c) Raman spectra for Calyx and Medulla/Cortex (red tissue).

future work, we will seek to increase the accuracy of the system and conducting additional trials on animal model in the process of carrying out human trials.

References

1. Aubertin, K., Trinh, V.Q., Jermyn, M., et al.: Mesoscopic characterization of prostate cancer using raman spectroscopy: potential for diagnostics and therapeutics
2. Bjurlin, M.A., Wysock, J.S., Taneja, S.S.: Optimization of prostate biopsy: Review of technique and complications. Urologic Clinics of NA **41**(2), 299 – 313 (2014)
3. Crow, P., Molckovsky, A., Stone, N., et al.: Assessment of fiberoptic near-infrared raman spectroscopy for diagnosis of bladder and prostate cancer. Urology **65**(6), 1126–1130 (2005)
4. Desroches, J., Jermyn, M., Pinto, M., et al.: A new method using raman spectroscopy for in vivo targeted brain cancer tissue biopsy. Scientific reports **8**(1), 1792 (2018)
5. Epstein, J.I., Feng, Z., Trock, B.J., Pierorazio, P.M.: Upgrading and downgrading of prostate cancer from biopsy to radical prostatectomy: Incidence and predictive factors using the modified gleason grading system and factoring in tertiary grades. European Urology **61**(5), 1019 – 1024 (2012)
6. Iping P, I.E., Day, J.C.C., Fullwood, L.M., Gardner, B., Stone, N.: Characterisation of a fibre optic raman probe within a hypodermic needle. Analytical and Bioanalytical Chemistry **407**(27), 8311–8320 (Nov 2015)
7. Jermyn, M., Mercier, J., Aubertin, K., et al.: Highly accurate detection of cancer in situ with intraoperative, label-free, multimodal optical spectroscopy. Cancer Research **77**(14), 3942–3950 (2017)
8. Poulin, E., Boudam, K., Pinter, C., et al.: Validation of mri to trus registration for high-dose-rate prostate brachytherapy. Brachytherapy **17**(2), 283 – 290 (2018)
9. Wang, L., He, D., Zeng, J., et al.: Raman spectroscopy, a potential tool in diagnosis and prognosis of castration-resistant prostate cancer. Journal of biomedical optics **18**(8), 087001 (2013)